Conference materials
UDC 537.9
DOI: https://doi.org/10.18721/JPM.161.132

Interconnect elements of magnonic networks based on controlled meander 3D magnonic structures

A.A. Martyshkin [1], Y.A. Gubanova [1]✉, E.N. Beginin [1], A.V. Sadovnikov [1]

[1] Saratov State University, Saratov, Russia

✉ yulya29022095@gmail.com

Abstract. Here we propose the different simple building block of the three-dimensional (3D) magnonic network in the form of the joined orthogonal sections of magnonic waveguides. It was shown, that the proposed 3D structures allows the transmission of spin-wave signals in the regime of surface magnetostatic wave propagation without the significant losses due to the junction region. Micromagnetic simulation was used to reveal the mechanism of spin-wave propagation across 3D junction. An electrodynamic problem is considered by the finite element method and the dispersion characteristics of spin waves (SW) are constructed with a change in the geometric parameters of the meander. The nature of the change in the frequency ranges of the Bragg band gaps depending on the meander profile has been studied in detail. It was demonstrated that spin-wave waveguiding 3D structure with broken translational symmetry exploiting the vertical spin-wave transport provides the transmission of the information signal in three-dimensional configuration of magnonic networks.

Keywords: Spin wave, micromagnetic calculation, 3D structure, Brillouin-spectroscopy

Funding: Ministry of Education and Science of the Russian Federation as part of the state assignment (project No. FSRR-2023-0008).

Citation: Martyshkin A.A., Gubanova Y.A., Beginin E.N., Sadovnikov A.V., Interconnect elements of magnonic networks based on controlled meander 3D magnonic structures. St. Petersburg State Polytechnical University Journal. Physics and Mathematics. 16 (1.1) (2023) 185–190. DOI: https://doi.org/10.18721/JPM.161.132

Материалы конференции
УДК 537.9
DOI: https://doi.org/10.18721/JPM.161.132

Элементы межсоединений магнонных сетей на основе управляемых меандровых 3D-магнонных структур

А.А. Мартышкин [1], Ю.А. Губанова [1]✉, Е.Н. Бегинин [1] , А.В. Садовников [1]

[1] Саратовский национальный исследовательский государственный университет имени Н.Г. Чернышевского, г. Саратов, Россия

✉ yulya29022095@gmail.com

Аннотация. В работе исследованы различные элементы трехмерной (3D) магнонной сети в виде соединенных ортогональных секций магнонных волноводов. Было показано, что предложенные 3D структуры позволяют передавать спин-волновые сигналы в режиме распространения поверхностных магнитостатических волн без потерь в нерегулярной области структуры. Для выявления механизма распространения спиновых волн через 3D-переход использовалось микромагнитное моделирование. Методом конечных элементов рассмотрена электродинамическая задача и построены дисперсионные характеристики спиновых волн (СВ) при изменении геометрических параметров меандра. Подробно изучен характер изменения частотных диапазонов брэгговских запрещенных зон в зависимости от профиля меандра. Продемонстрировано, что спин-волновая 3D-структура с нарушением трансляционной симметрией, использующей вертикальный спин-волновой транспорт, обеспечивает передачу информационного сигнала в трехмерной конфигурации магнонных сетей.

Ключевые слова: Спиновые волны, микромагнитное моделирование, трехмерные структуры, Мандельштам-бриллюэновская спектроскопия

Финансирование: Минобрнауки России в рамках выполнения государственного задания (проект № FSRR-2023-0008).

Ссылка при цитировании: Мартышкин А.А., Губанова Ю.А., Бегинин Е.Н., Садовников А.В. Элементы межсоединений магнонных сетей на основе управляемых меандровых 3D-магнонных структур // Научно-технические ведомости СПбГПУ. Физико-математические науки. 2023. Т. 16. № 1.1. С. 185–190. DOI: https://doi.org/10.18721/ JPM.161.132

Introduction

The transition from a two-dimensional architecture of magnon networks to a three-dimensional one is currently of great interest due to the development of data processing and storage concepts based on magnonic principles [1]. In electronics, 3D circuits require efficient removal of Joule heat from computational elements, which is a technological challenge. Magnonics allows you to transmit an information signal encoded in the amplitude and phase of spin waves (SW), while the transport properties of spin-polarized electrons are not used, and information is transferred by signal transmission using spin wave [2]. With this approach, it is possible to implement a number of signal processing functional blocks with low power consumption compatible with semiconductor electronic circuits and the possibility of miniaturization to nanometer sizes of structures [3].

One of the options for creating interconnect elements based on magnetic quasi-two-dimensional and three-dimensional (3D) structures in lateral and vertical topologies with micro- and nanometer-sized waveguide elements is a base element made in the form of ferrite microwave guides located on the same substrate and connected through the side wall [4]. In this case, the interconnections will perform not only the transmission of the information signal, but also functional processing, implementing the modes of parallel and multi-stream (de)multiplexing of the spin-wave signal in the frequency, time and space domains. Most circuits based on magnon logic are magnetized in a plane, which imposes restrictions on signal routing, since magnon networks limited to one functional level have a critical signal propagation length and a large device area [5]. Structures with the possibility of vertical transport of a spin-wave signal [6] make it possible to create three-dimensional magnon networks (MS) with a large number of functional blocks in a smaller volume.

Meander-type ferromagnetic films grown on the surface of periodically structured substrates can be considered as a three-dimensional magnonic crystal structure. Composite magnon crystals are in fact magnonic metamaterials with periodically varying parameters that exhibit SW delay control, and analysis of the dispersion response of such structures indicates that the SW spectrum can be divided into periodically alternating frequency bands in which SW propagation is observed (passbands), and frequency bands in which no SW propagation occurs due to additional attenuation arising from Bragg interference of incident and reflected waves. The formation of such band gaps in the magnon spectrum makes it possible to use MCs as filters for the SW signal. The study of MC with different periodicity in one and two dimensions [7] led to the development of the field of magnonics [8].

The 3D structures considered in this paper can be used as interconnection elements for multilayer topologies of magnon networks that perform the functions of information signal processing [9].

Vertical interconnection elements of 3D magnonic networks

We investigate vertical transport of spin waves in two structures shown in Fig. 1, *a*, *b*. The structure in the form of an orthogonal connection of two magnetic thin-film sections S_1 and

S_2 is shown in Fig. 1, *a*. A stepped structure consisting of the connection of three separate sections S_3, S_4 and S_5 is shown in Fig. 1, *b*. Thin film yttrium iron garnet (YIG) [$Y_3Fe_5O_{12}$ (111)] 1 μm thick and saturation magnetization M_0 = 1.39×10^5 A/m on a gallium-gadolinium garnet substrate 500 μm thick (GGG) [$Gd_3Ga_5O_{12}$ (111)]. YIG film exchange constant was taken equal to A_{ex} = 3.614×10^{-12} J/m. Waveguide width in the numerical calculation w = 100 μm was changed to the case of a transversely limitless YIG film. The length of the waveguides S_1, S_2 was $L_1 = L_2$ = 1000 μm. The structures were placed in an external magnetic field H_0 = 1200 Oe directed along the *y*-axis to effectively excite a magnetostatic surface spin wave (MSSW) in the S_1 region [10]. The stepped structure shown in Fig. 1, *b* is formed by sections $S_3 = S_4 = S_5$ with length $L_3 = L_4 = L_5$ = 1000 μm.

To investigate the properties of propagation of a spin-wave signal in the investigated structures with broken translational symmetry, we used the method of numerical micromagnetic simulations based on a numerical solution of the Landau–Lifshitz–Gilbert equation [11, 12]:

$$\frac{\partial \vec{M}}{\partial t} = \gamma\left[\vec{H}_{eff} \times \vec{M}\right] + \frac{\alpha}{M_0}\left[\vec{M} \times \frac{\partial \vec{M}}{\partial t}\right],$$

where $\vec{M}$ is the magnetization vector, α = 10^{-5} is the damping parameter, $\vec{H}_{eff} = -\frac{\delta E}{\delta \vec{M}}$ is the effective magnetic field, ***E*** is the free energy of the magnet. The contribution of magnetocrystalline anisotropy in the plane of the film in view of its smallness can be neglected. To reduce the signal reflections from the boundaries of the computational domain in numerical simulation, two regions at the beginning and end of the waveguide with a low damping parameter α decreasing in geometrical progression from α = 10^{-5} to α = 10^{-1}.

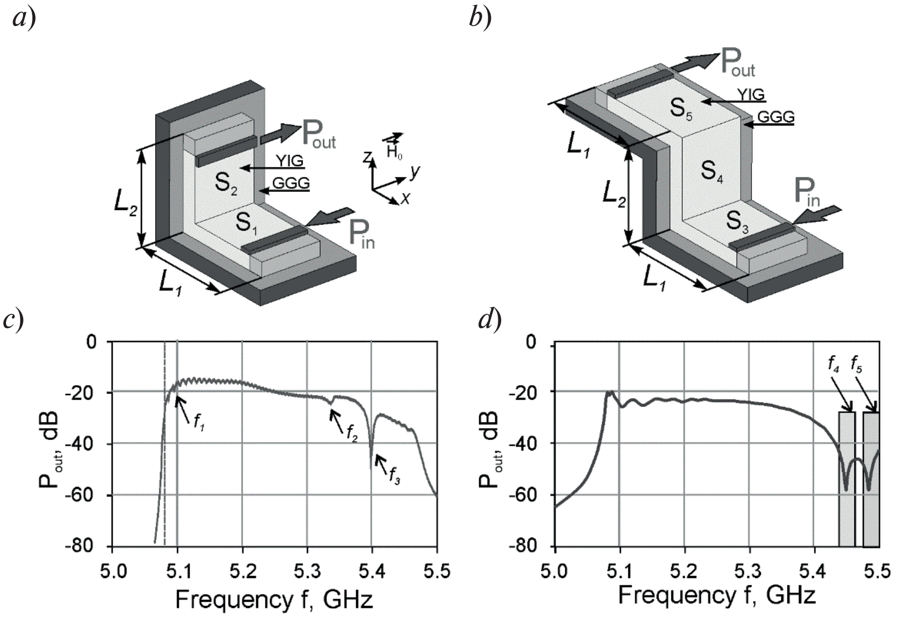

Fig. 1. Schematic view of interconnect element in the form of an L-shaped (*a*) and step-shaped (*b*) junction of magnetic films; the transmission spectrum of the output signal for the *L*-shaped (*c*) and for step-shaped (*d*) structure

To calculate the output signal spectrum, the problem of excitation of a SW was solved for the *L*-shaped structure using the excitation method in the region of the microwave S_1 and receiving the SW in the waveguide S_2. The SW excitation in the numerical counting was carried out by setting the value of the alternating magnetic field in the form $B_x(t) = b_0\mathrm{sinc}(2\pi f_0(t-t_0))$, where b_0 = 10^{-3} *T*, f_0 = 4 GHz, t_0 = 0.1 ns.

The frequency spectrum of such a function has a rectangular shape with a cut-off frequency f_0. The source was localized in the signal source region inside the waveguide, the size of which was 5 μm in the direction of the *x*-axis. This method of excitation is close to the standard excitation of microwave oscillations of magnetization using a microstrip antenna with a thickness of 2 μm and a width of 5 μm located on the surface of the YIG film [13]. After the excitation of the pulse, the magnetization behavior of time was fixed for T_m = 300 ns. Then the array of obtained data was subjected to Fourier transform and as a result, the output signal spectrum was obtained for the reference structure and the *L*-shaped microwave guide under study. Fig. 1, *c* shows the results of calculating the spectrum of the spin-wave signal in the output section of microwave S_2 of an investigated irregular structure with broken translational symmetry. The beginning of the frequency bandwidth of the structures under study corresponds to the frequency $f_0 = \sqrt{f_H(f_H+f_M)}$ = 5.096 GHz, where $f_H = \gamma H_0$, $f_M = \gamma\mu M_0$, γ is the gyromagnetic ratio for YIG.

At the frequencies f_2 and f_3, the irregularity region is the source of short dipole-exchange waves [14] due to the presence of a gradient of the internal magnetic field in the region of the bending of the *L*-shaped microstructure. This mechanism for generating short SWs in this case can explain the characteristic dips in the output power spectrum (Fig. 1, *d*) at frequencies f_2 and f_3. As shown in [15], MSSWs propagating along the *x*-axis are weakly reflected from the joints of the vertical and horizontal segments.

The origin of multiple dips in the shaded region in Fig. 1, *d* denoted with f_4 and f_5 can be originated from inhomogeneous magnetic field in the double junction region in the case of step-shaped junction (Fig. 1, *b*) in comparison with *L*-shaped structure (Fig. 1, *a*). The conditions for short spin wave generation in the former case are originated from the non-uniform distribution of the internal magnetic field in the two regions: junction of section S_5 and S_4; junction of section S_4 and S_3. The detailed mechanism of this dips formation are beyond the current manuscript.

Control of band gaps in three-dimensional meander structures

Combining *L*-shaped interconnect elements into a meander array makes it possible to avoid the limitations associated with attempts to control SW [16], which are difficult to implement using plane magnetized films due to the anisotropic dispersion of SW, which depends on the relative orientation of the magnetization and the wave vector.

Figure 2, *a* shows a segment of a periodic 3D magnon YIG structure in cross section used to simulate a meander structure with the following parameters: modulation period *L* = 740 nm, height of the lower horizontal sections m_1 = 50 nm, height of the upper horizontal sections m_2 = 50 nm, thickness of the vertical sections m_3 = 50 nm, drop height *p* = 120 nm. The direction of the external magnetic field was directed along the *z*-axis.

Numerical simulation was carried out by solving the system of Maxwell equations by the finite element method in the COMSOL Multiphysics software product. The calculation of the dispersion characteristics was carried out considering the fact that the components of the electromagnetic field depended on the frequency according to the harmonic law. The equation for the electric field strength vector ***E*** had the following form:

$$\nabla \times (\hat{\mu}^{-1} \nabla \times \mathbf{E}) - k^2 \varepsilon \mathbf{E} = 0$$

where $k = \omega/c$ is the wave number in vacuum, $\omega = 2\pi/f$ is the circular frequency, *f* is the frequency of the electromagnetic wave, and ε is the effective value of the permittivity. In this case, the magnetic permeability tensor for tangential magnetization has the form:

$$\hat{\mu} = \begin{vmatrix} \mu(f) & -i\mu_a(f) & 0 \\ i\mu_a(f) & \mu(f) & 0 \\ 0 & 0 & 1 \end{vmatrix},$$

$$\mu(f) = \frac{-f_B(f_B + f_M) - f^2}{f_B^2 - f^2},$$

$$\mu_a(f) = \frac{f_M f}{f_B^2 - f^2}.$$

It should be noted that this method makes it possible to make calculations considering the non-single-year distribution of the internal magnetic field.

As a result of numerical simulation, dispersion characteristics were obtained for direct and

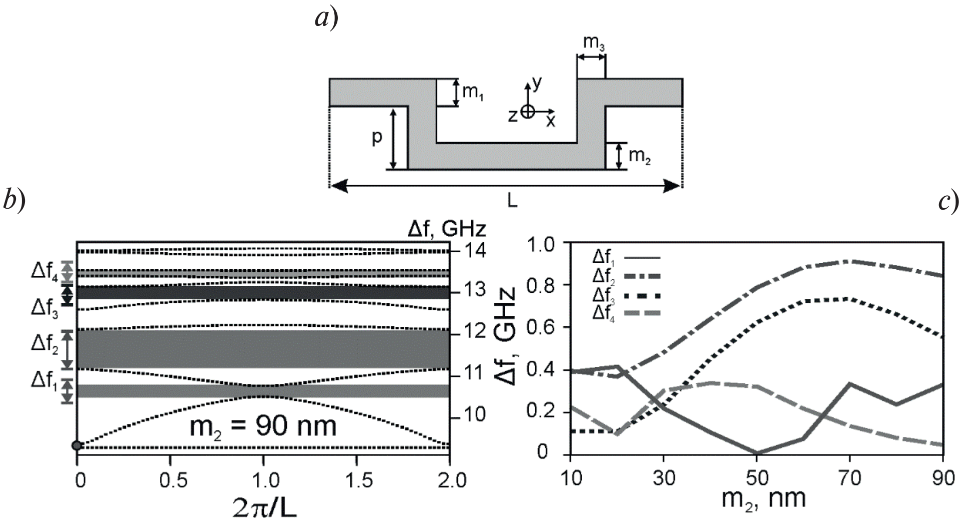

Fig. 2. Schematic view of the meander structure (*a*), dispersion characteristic at m_2 = 90 nm (*b*), dependence of the frequency ranges of the Bragg band gaps on the change in the drop height *p* (*c*)

counterpropagating waves with a section width m_2 = 90 nm (Fig. 2, *b*). On the dispersion characteristics, one can see the frequency ranges of the Bragg band gaps in which the propagation of spin waves is impossible. It can be seen that at m_2 = 90 nm in the frequency range Δf_1 in the SW spectrum, the first band gap is formed (near the wave number $k \sim k_B = 2\pi/L$). The color on the dispersion characteristics indicates the frequency ranges of the Bragg band gaps. In this case, the frequency band gap has the greatest value for the low-frequency mode in the region Δf_2 for waves with a wave number near $k \sim 2k_B$. The next band gap is formed for SW with a wave number near $k \sim 2k_B$, its width is denoted by Δf_3. For the blocking zone for SW with a wave number near $k \sim 4k_B$, the designation Δf_4 is introduced.

To analyze the effect of a change in the thickness of the vertical sections m_2 on the nature of the dispersion characteristic, the value of m_2 took a value from 10 to 90 nm. As a result, it was found that at $k = 1$ it is possible to control the widths of the Bragg band gaps.

Fig. 2, *c* shows the dependence of frequency ranges of SW non-transmission on the parameter m_2 for four bands Δf_1, Δf_2 and Δf_3, Δf_4 (solid, dashed-dotted, dashed and dotted respectively). The horizontal segment thickness parameter m_2 was varied in the range from 10 nm to 90 nm. The thickness of the ferromagnetic layer in the vertical section was m_3 = 25 nm, and the difference *p* =100 nm. At the value of the parameter m_2 = 50 nm, the value of the frequency range of the first band gup, for waves with a wave number near $k \sim k_B$, is maximum and is 0.42 GHz. However, for SW with a wave number near $k \sim 2k_B$ and $k \sim 4k_B$, the maximum value of the frequency band gap width is observed at approximately m ~ 70 nm. For SW with a wave number near $k \sim 6k_B$ at parameter values m_2 ~ 90 nm, the value of the frequency band gap is minimal. Near these values of the parameter m_2 ~ 50 nm, the band gap Δf_1 is closed.

This means that in the vicinity of these values *p* of the parameter m_2 one can observe the closure of the band gap Δf_1. By varying the meander modulation depth, it is possible to control the width of the non-transmission frequency band in the spectrum of spin waves propagating in a meander structure, which can be used in the design and manufacture of microwave filters based on nanoscale magnon-crystalline structures made in the form of meander ferromagnetic films.

REFERENCES

1. **Nikitov S.A., Safin A.R., Kalyabin D.V. et al.,** Dielectric magnonics: from gigahertz to terahertz, Physics–Uspekhi. 10 (63) (2020) 945–974.

2. **Allwood D.A., Xiong G., Faulkner C.C., Atkinson D., Petit D, Cowburn R.P.,** Magnetic domain-wall logic. Science. 309 (5741) (2005) 1688-1692.

3. **Barman A., Gubbiotti G., Ladak S., Adeyeye A.O., Krawczyk M., Gräfe J., Winklhofer M.,** The 2021 magnonics roadmap. Journal of Physics: Condensed Matter, 33 (41) (2021) 413001.

4. **Sadovnikov A.V., Beginin E.N., Sheshukova S.E., Romanenko D.V., Sharaevskii Yu.P., Nikitov S.A.,** Directional multimode coupler for planar magnonics: Side-coupled magnetic stripes. Applied Physics Letters, 107 (20) (2015) 202405.

5. **Niemier M.T., Bernstein G.H., Csaba G., Dingler A., Hu X.S., Kurtz S., Liu S., Nahas J., Porod W., Siddiq M., Varga E.,** Nanomagnet logic: progress toward system-level integration. Journal of Physics: Condensed Matter, 23 (49) (2011) 493202.

6. **Martyshkin A.A., Beginin E.N., Stognij A.I., Nikitov S.A., Sadovnikov A.V.,** Vertical spin-wave transport in magnonic waveguides with broken translation symmetry. IEEE Magnetics Letters, 10 (2019) 1–5.

7. **Nikitov S.A., Tailhades Ph., Tsai C.S.,** Spin waves in periodic magnetic structures—magnonic crystals. Journal of Magnetism and Magnetic Materials, 236 (3) (2001) 320-330 2001.

8. **Chumak A.V., Serga A.A., Hillebrands B.,** Magnonic crystals for data processing. Journal of Physics D: Applied Physics, 50(24) (2017) 244001.

9. **Beginin E.N. et. al.,** Three-Dimensional Magnonics CRC Press.

10. **Damon W., Eshbach J.R. Damon, R.W. & Eshbach J.R.,** Magnetostatic modes of a ferromagnet slab. Journal of Physics and Chemistry of Solids, 19 (3-4) (1961) 308-320.

11. **Landau L.D., Lifschitz E.M.,** Phys. Z. Sowjet, 8 (153) (1935).

12. **Vansteenkiste A., Leliaert J., Dvornik M., Helsen M., Garcia-Sanchez F., Waeyenberge B., Garcia-Sanchez F., & Van Waeyenberge B.,** The design and verification of MuMax3. AIP advances, 4 (10) (2014) 107133.

13. **Sadovnikov A.V., Grachev A.A., Sheshukova S.E., Sharaevskii Yu.P., Serdobintsev A.A., Mitin D.M., Nikitov S.A.,** Magnon straintronics: Reconfigurable spin-wave routing in strain-controlled bilateral magnetic stripes. Physical review letters, 120 (25) (2018) 257203.

14. **Davies C.S., Francis A., Sadovnikov A.V., Chertopalov S.V., Bryan M.T., Grishin S.V., Allwood D.A., Sharaevskii Y.P., Nikitov S.A., Kruglyak V.V.,** Towards graded-index magnonics: Steering spin waves in magnonic networks. Physical Review B, 92 (2) (2015) 020408.

15. **Beginin E.N., Sadovnikov A.V., Sharaevskaya A.Y., Stognij A.I., Nikitov S.A.,** Spin wave steering in three-dimensional magnonic networks. Applied Physics Letters, 112(12) (2018) 122404.

16. **Vogt K., Fradin F.Y., Pearson J.E., Sebastian T., Bader S.D., Hillebrands B., Hoffmann A., Schultheiss H.,** Realization of a spin-wave multiplexer. Nature communications, 5 (1) (2014) 1–5.

THE AUTHORS

MARTYSHKIN Alexandr A.
aamartyshkin@gmail.com

BEGININ Eugeny N.
egbegin@gmail.com

GUBANOVA Yulya A.
yulya29022095@gmail.com

SADOVNIKOV Alexandr V.
sadovnikovav@gmail.com

Received 30.10.2022. Approved after reviewing 24.03.2023. Accepted 24.03.2023.